Since January 2020 Elsevier has created a COVID-19 resource centre with free information in English and Mandarin on the novel coronavirus COVID-19. The COVID-19 resource centre is hosted on Elsevier Connect, the company's public news and information website.

Chemical Engineering Journal 260 (2015) 801–808

Contents lists available at ScienceDirect

Chemical Engineering Journal

journal homepage: www.elsevier.com/locate/cej

Synthesis of hybrid hydrophobic composite air filtration membranes for antibacterial activity and chemical detoxification with high particulate filtration efficiency (PFE)

Anbharasi Vanangamudi, Sakinah Hamzah, Gurdev Singh *

Environmental & Water Technology Centre of Innovation, Ngee Ann Polytechnic, Singapore 599489, Singapore

HIGHLIGHTS

- Nanofiber filters incorporated with Al_2O_3 nanoparticles were prepared for air filtration.
- The filters are antibacterial, detoxifying and with excellent particle filtration efficiency.
- Detoxification efficiency of filter to paraoxon increased with higher Al_2O_3 concentrations.
- Particle filtration efficiency of filters also increased with higher Al_2O_3 concentrations.
- Resistance of filters only increased marginally with higher Al_2O_3 concentrations.

GRAPHICAL ABSTRACT

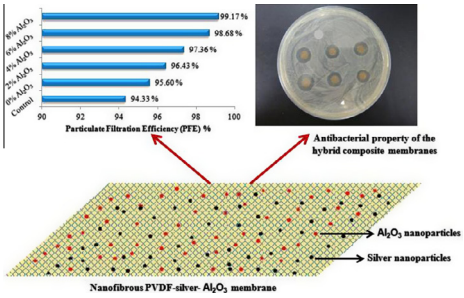

ARTICLE INFO

Article history:
Received 25 April 2014
Received in revised form 6 August 2014
Accepted 15 August 2014
Available online 17 September 2014

Keywords:
Electrospinning
Particulate filtration efficiency (PFE)
Antibacterial activity
Chemical detoxification
Composite hydrophobic membrane
Air filtration membranes

ABSTRACT

Hybrid hydrophobic composite PVDF–Ag–Al_2O_3 nanofibrous air filtration membranes are synthesized by the electrospinning method with different concentrations of Al_2O_3 and fixed concentration of Ag to study their antibacterial, particulate filtration efficiencies, and their detoxification ability. All the membranes were characterized for their physical and chemical properties before being tested. It was also found that at Al_2O_3 concentrations higher than 8%, nanofibers could not be formed by the pure blending and electrospinning technique. The antibacterial activity of the membranes proved that silver incorporation provided suitable disinfection with greater than 99.5% antibacterial efficiency for all membranes. The antibacterial efficiency of the membranes was maintained even as the concentration of Al_2O_3 was increased. The hydrolysis of paraoxon, a nerve agent simulant, for the prepared membranes was also studied. The removal of paraoxon was found to increase as the loaded concentration of Al_2O_3 in the membrane increased. The particulate filtration efficiency of the prepared membranes was tested using particles of diameter 0.36 μm. Compared to the nascent PVDF nanofiber membranes with particle filtration efficiency of 94%, the Ag and Al_2O_3 loaded membranes all had a higher particle filtration efficiency. Interestingly, it was found that as the concentration of Al_2O_3 loaded in the membranes increased so did the particle filtration efficiency. Membrane characterization data revealed that as the concentration of the Al_2O_3 was increased, the average pore size of the membrane was reduced and the thickness of the filter mat increased. This would explain the higher retention of the particles by

* Corresponding author at: Environmental & Water Technology Centre of Innovation, Ngee Ann Polytechnic, Singapore, Blk 39, #01-06, 535 Clementi Road, Singapore 599489, Singapore. Tel.: +65 6460 7511; fax: +65 6467 4185.
E-mail address: gurdev@np.edu.sg (G. Singh).

http://dx.doi.org/10.1016/j.cej.2014.08.062
1385-8947/

these filters. Correspondingly, the resistance of the filters also increased as more Al_2O_3 was loaded in the nanofiber membranes. The synthesized nanofibrous membranes have the potential to be used as 3 in 1 highly efficient air filters.

1. Introduction

Air pollution poses a serious health threat. Technologies that provide protection from contaminants or remove them are becoming more important both for industry and the general public. There are several contaminants in air that can adversely affect health and need to be addressed.

Particulate matter comprising either of solid particles and/or liquid droplets of different sizes is a major source of pollution. The common classification for particulate matter is PM10 (referring to coarse particulate matter of size ranging from 2.5 to 10 μm), PM2.5 (fine particulate matter of size ranging from 0.1 to 2.5 μm) and PM0.1 (ultrafine particulate matter of size below 0.1 μm). Increasingly, greater emphasis is being paid on PM2.5 due to its serious health implications [1–3]. Removal of particulate matter is commonly achieved through the use of porous filters. In addition to particulate matter, other harmful chemicals and biological contaminants in air also need to be addressed. It will be ideal if air filters could also address other contaminants besides particulate matter.

Besides particulate matter, biological matter such as bacteria and viruses can also impact health and this was evident with the recent outbreaks of the Severe Acute Respiratory Syndrome (SARS) and Middle Eastern Respiratory Syndrome (MERS). Silver, over the years has been used in various anti-microbial applications from water treatment, healthcare and bioengineering [4–8]. Silver nanoparticles have also been found to be highly effective disinfectants to many bacteria and viruses due to its small size [9–12]. Besides silver, some metal oxides have also been found to have disinfecting properties. Metal oxides such as ZnO are reported to be used in antibacterial cream, lotions and ointments [13]. CuO has been found to express activity against bacterial pathogens such as methicillin resistant strain of *Staphylococcus aureus* and *Escherichia coli* [14]. The combination of silver with metal oxides has also been shown to enhance disinfection performance. A recent study reporting the combination of silver and silver bromide nanoparticles further enhanced the antimicrobial activity of TiO_2 [15,16].

Other pollutants such as chemicals could also pose risks. On the extreme end of the spectrum, chemical warfare agents such as nerve gas, mustard agent, blood agents and toxins such as arsine pose a serious health risk. These chemical contaminants are broadly characterized as organophosphorus (OP) nerve agents, which break down the acetylcholine, a neurotransmitter located at the nerve endings [17–24]. Paraoxon, is an example of a chemical warfare agent simulant which is widely used as a pesticides [23]. A method used by the military to combat these chemical contaminants in air is to pass the air through a liquid known as DS2 comprising of 2% NaOH, 28% 2-methoxyethanol and 70% diethylene triamine [25]. Other solutions to remove chemical contaminants from air are through adsorption with activated carbon or other carbon based materials being employed. More recently, nano-silver and other metal oxide nanoparticles such as ZnO, CuO, TiO_2, were found to hydrolyze these chemical contaminants through the Lewis and Bronsted and the acidic sites [26–28]. Other studies have also confirmed that the use of metal oxide nanoparticles such as Al_2O_3, Fe_2O_3, TiO_2 and MgO could serve as an effective catalyst against chemical warfare agents [29–31] and potentially other chemicals in air as well.

In this paper, we report the development of hybrid composite nanofibrous air filtration membrane that is able to effectively remove pollutants in air such as particulate matter, biological contaminants as well as chemical pollutants in a single step through filtration. More importantly, we have developed a filter that is able to achieve high contaminant removal rates, while also allowing high mass transfer through it or low resistance. This is critical, as better protection is typically achieved at the expense of higher energy to push air through the filter. To achieve this, we have worked with nanofibers, which have been shown to have smaller resistance when compared to spun-bound or melt blown microfibers that are commonly used for air filtration [32]. More specifically, air filters comprising of PVDF nanofibers, blended with silver and aluminum oxide nanoparticles were produced by electrospinning. The produced filters were characterized and studied for their effectiveness in removing particulate matter; bacteria and a model OP compound i.e. paraoxon.

2. Materials and methods

2.1. Materials

PVDF Kynar® 761 grade with a melting point of 165–172 °C was purchased from Arkema Pte., Ltd., Singapore. Silver nitrate ($AgNO_3$) 99.8% and aluminum oxide nanopowder (melting point 2040 °C) of particle size 13 nm with BET surface area of 85–115 m^2/g was purchased from Sigma Aldrich, Singapore. Paraoxon (diethyl p-nitrophenyl phosphate, Sigma, Singapore) was used as received. Dimethyl formamide (DMF), acetone and N, N′ dimethyl acetamide (DMAC) were analytical grade from Sigma, Singapore as well. The deionized water used was distilled and purified with a Milli-Q plus system from Millipore, Bedford, MA, USA.

2.2. Synthesis of hybrid PVDF–Ag–metal oxide hydrophobic membranes

15% PVDF solution was prepared using DMAC and acetone in the ratio 2:3 respectively. Silver nanoparticles were fabricated using a simple method and has been used along with the polymer to prepare a homogenous solution [33]. First, $AgNO_3$ (0.83 g) was dissolved in DMF solvent until the solution turns brownish indicating that the silver nitrate has been reduced to silver (Ag) nanoparticles due to the presence of DMF, that acts as an active reducing agent in the absence of protecting agent under suitable conditions [34]. After complete dissolution of the polymer, the reduced blackish silver nanoparticle solution is added to 15% PVDF solution. The solution was allowed to stir until it become homogenous. To this solution, 0%, 2%, 4%, 6% and 8% Al_2O_3 was added individually and stirred well. The solutions were kept for stirring at 70 °C for 1 h, then at room temperature for 48 h and were found to change color gradually. The PVDF–Ag–Al_2O_3 solutions were found to be blackish-brown.

The different PVDF–Ag–Al_2O_3 membranes, M1 (using 0% Al_2O_3), M2 (using 2% Al_2O_3), M3 (using 4% Al_2O_3), M4 (using 6% Al_2O_3), M5 (using 8% Al_2O_3) using different concentrations of Al_2O_3 and same concentration of silver nanoparticle solution were prepared by electrospinning the prepared homogenous solutions of PVDF–

Ag–Al_2O_3 with 0, 2, 4, 6, 8% Al_2O_3. 15% PVDF in DMAC and acetone (2:3) is electrospun and used as a control. 10 mL of the polymer solution was electro-spun at a rate of 2 mL/hr by applying a high voltage of 30 kV between the tip of the spinneret and the rotating metal drum (collector), to get a uniform thickness. After electrospinning, the nanofibrous metal oxide membranes (M1, M2, M3, M4, M5 and control) are dried for a day at room temperature for the solvents to evaporate. The dried membrane was heat treated (post treatment) at 135 °C for 15–20 min. The silver nanoparticles on the surface of the nanofibers were found to increase upon treating with UV light [35]. Thus, the membranes were kept under UV light for about 20 min to make sure that all the silver nitrate is photoreduced to silver nanoparticles [36], which can be observed by the color change of the membranes from yellow to brownish black. The concentration of Al_2O_3 cannot go beyond 8% for 15% PVDF. This is because for more than 8% Al_2O_3 the viscosity increases to an extent where the solution cannot be electrospun. Thus, for 15% PVDF solution, the maximum electrospinnable Al_2O_3 concentration is 8%.

2.3. Characterization

The membranes were characterized using Fourier Emission Scanning Electron Microscopy (FESEM) to observe the morphology of the samples. The samples were sputter coated with platinum, using a JFC-1600 auto fine coater (JOEL, Tokyo Japan) and the morphology was observed by using FESEM (JOEL JMS-6400, Japan) at different magnifications to calculate the diameter of the fibers. The presence of nanoparticles was confirmed using the energy dispersive X-ray (EDX) analysis.

The membranes were also characterized for its thickness using the micrometer screw gauge (Mitutoyo, Japan) and pore size using the capillary flow porometer (Quantochrome 3G zh, USA).

The water contact angles (CA) of the membranes were determined using the VCA Optima Surface Analysis System (AST Products, Inc., Billerica, MA, USA) to study their hydro-phobicity/-philicity. Samples of 4 cm^2 area (2 × 2 cm) at random positions were prepared from each membrane. The samples were then placed on the glass sample plate and fixed with tape. The equipment syringe filled with distilled water was installed to stand vertically. 1 μl was deposited on the membrane surface. The CA was measured at 3 different points on each membrane sample.

2.4. Evaluation of antibacterial activity

The antibacterial activity of the membranes and the control was determined by two methods namely the qualitative (Zone Inhibition test) and the quantitative (antibacterial efficiency test) method similar to the one done by Guangtao Li et al. [37]. Here, *E. coli* was used as testing organism to investigate the membranes. Before testing, all materials were autoclaved at 121 °C for 20 min to ensure sterility. *E. coli* was cultivated using the Luria–Bertani (LB) broth and incubated overnight at 37 °C in a shaker.

2.4.1. Zone Inhibition test

For the qualitative evaluation, nutrient agar is poured onto the disposable sterilized petri dishes and was allowed to solidify. 100 μl of 5×10^7 CFU/ml *E. coli* concentrations was streaked over the culture plate and was spread uniformly. The membranes were cut according to the size of the Kirby–Bauer disk (6 mm in diameter). The membrane and the control samples were placed gently over the solidified agar plate and were spaced out in the petridish. The plate was incubated at 37 °C for overnight and was observed. The antibacterial activity was identified and estimated by a clear zone of inhibition.

2.4.2. Antibacterial efficiency test

The inoculums of *E. coli* were prepared by growing strains in LB medium at 37 °C until a level of approximately 5×10^7 CFU/mL. The membrane samples (of known weight) were introduced into the LB broth solution containing 5×10^7 CFU/10 mL of *E. coli*. The sample membranes and the control were cultured at 37 °C in a shaker incubator for about 5–6 h at 250 rpm followed by 10 times of 10× serial dilution with the LB broth. 100 μl of the overnight culture and each dilution were spread uniformly on solidified agar plates. Plates were incubated at 37 °C overnight. The number of bacterial colonies (CFU) was counted with the SC6 STUART® colony counter to determine the antimicrobial effect. The percentage efficiency was calculated using the formula, % efficiency = $(C - T)/C \times 100$, where C = CFUs of the original culture for the test control; T = CFUs of the original culture for the test sample.

2.5. Detoxification studies

The membranes were evaluated for their ability to detoxify Paraoxon, a model chemical pollutant used in this study. Briefly, 7.5 μl of paraoxon (as received) was diluted using heptanes to make a stock of 30 ppm. The intensity of the stock solution was noted at λ_{max} = 268 nm using a UV spectrophotometer (Model UV-1800 from Shimadzu). 25 ml of this solution was added to 30 cm^2 of membrane. The solution was tested at 1 min intervals for 10 min and then at 30, 60 and 120 min at λ_{max} = 268 nm. The control cuvette contained the paraoxon solution prior dipping the sample. The kinetics of hydrolysis was examined with the decrease in intensity of the solution. Here, the membranes were tested for paraoxon hydrolysis using a similar method as carried out previously [24].

2.6. Particulate filtration efficiency (PFE)

Fig. 1 shows the schematic of the experimental system for the measurement PFE throughout the membranes. This involves testing the membranes for particle filtration efficiency by passing submicron aerosol particles of DEHS oil at a particular concentration and measuring the concentration before (upstream) and after (downstream) passing through the membranes. The PFE of the membrane can be calculated from the leakage % given by the system. The test membrane was held in a filter holder that has effective testing area of about 20 cm^2. The test was conducted at a flow rate of about 32 L/min and a velocity of 26.67 cm/s. The upstream and the downstream concentration were measured using the ATI 2H digital photometer and is fed into the control system and then to the PC as the output.

2.7. Filter resistance

The resistance of the filter is an important parameter that determines the breathability of the filters. To determine the filter resistance, air was pushed through at a fixed flow rate and the difference in air pressure (ΔP) before and after the filter was measured. All tests were carried out at a fixed velocity (v) of 28.4 cm/s. The resistance of the filters (R_f) can then be calculated by filtration theory using the following equation:

$$R_f = \Delta P / v$$

where ΔP is the pressure drop of the filter and v is the velocity of air passing through the filter.

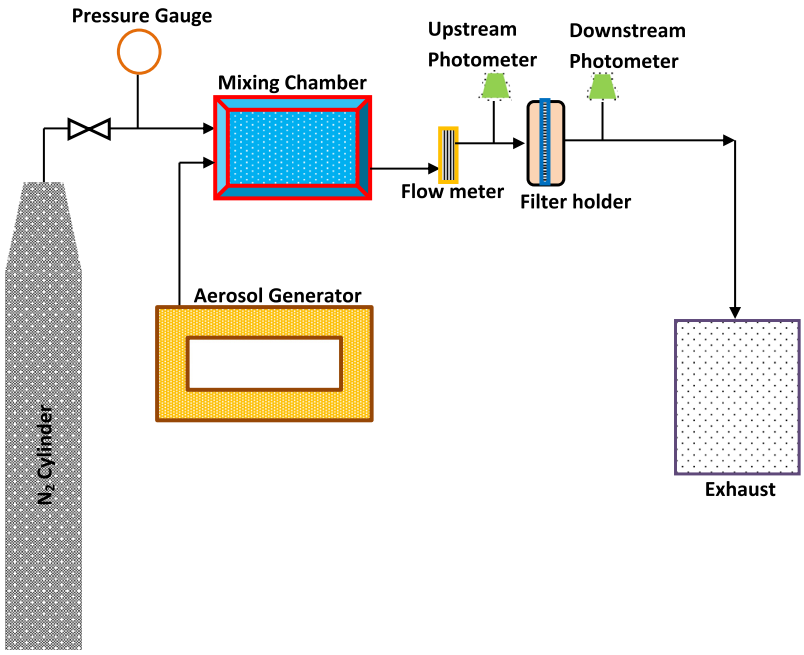

Fig. 1. Experimental set-up for testing particulate filtration efficiency (PFE).

3. Results and discussion

The nanofibrous hybrid PVDF–Ag–Al_2O_3 membranes for air filtration were prepared by mixing Al_2O_3 and silver nanoparticles with PVDF polymer solution and making it homogenous followed by electrospinning the solution. The antibacterial activity, detoxification efficiency and the PFE of the membranes were tested, studied and compared. Here, DMF is used as a solvent or co-solvent for dissolving silver nitrate, since it behaves as an active reducing agent forming silver nanoparticles at room temperature [33].

3.1. Characterization

Fig. 2 shows the FESEM images of the composite electrospun nanomembranes M1, M2, M3, M4 and M5 after the post treatment. The images resemble the nanofibers prepared with 15 wt% PVDF using DMAC/Acetone (2:3) as solvent observed by Matsuura and coworkers [38]. In addition to the fibers, we can also find the Al_2O_3 nanoparticles attached onto the nanofibers. The presence of Al_2O_3 nanoparticles on the surface of the membrane was confirmed by comparing EDX images of the membrane samples with nanoparticles. From the SEM images, we can visualize that the amount of Al_2O_3 in M5 is higher than the rest of the membranes and is confirmed by the EDX measurements. We can also see that the amount of silver is almost the same in all the EDX spectrums. This shows that the developed composite membranes contain Ag and Al_2O_3 nanoparticles, which can disinfect microorganisms and detoxify chemical pollutants respectively that come into contact with the membrane. The Java image processing software [Image J1.29 (222 commands)] was used to measure the diameter of the fibers from the SEM images. Table 1 shows the average membrane diameters of M1, M2, M3, M4 and M5. It was found that the fiber diameter is 0.85 μm for M5 which is higher than the rest of the membranes and might be due the presence of the increased metal oxide nanoparticles after post treatment as seen in the SEM images. Thus the increased orders of the fiber diameter of the membranes are found to be M1 < M2 < M3 < M4 < M5.

Table 1 shows the average thickness of the post treated membranes (M1, M2, M3, M4, M5 and control) measured using a micrometer screw gauge (Mitutoyo, Japan). From the table, we can observe that the average thickness of the membrane increases as the metal oxide composition increases and was found to be higher for the M5 (which has 8% Al_2O_3) i.e. 62.9 μm, where as for the PVDF (control) membrane it is 50.4 μm.

The static water contact angle (CA) of the membranes was measured at room temperature. A sessile drop of liquid (1.0 μ drop size) was placed on the surface of the membrane using a micro syringe. The average water CA ($n = 5$) of the electrospun nanofiber membranes were shown in Table 1. It was observed that the average CA of the composite membranes is almost same as the PVDF membrane which is about 139.4 ± 0.7°. This shows that the addition of Al_2O_3 nanoparticles does not affect largely the hydrophobicity of the nanofibrous membranes and that the developed membranes, being hydrophobic, are suitable for air filtration applications by avoiding moisture absorption on to the membrane and are air permeable. The increased hydrophobicity is due to the inherent surface roughness and trapped air pockets [39].

3.2. Evaluation of antibacterial activity

3.2.1. Zone Inhibition test

In the present work, the membranes M1, M2, M3, M4 and M5 exhibited positive results with PVDF as a control, which do not show any inhibition zone. Fig. 3 shows the zone of inhibition of the membrane samples and the control. All the membranes with silver cleared the *E. coli* bacteria around them and we observed distinct zones of inhibition (clear areas with no bacterial growth) around the membranes. The width of the zone around the control PVDF membrane, M1, M2, M3, M4 and M5 was about 0, 6.5, 6, 5, 5.5 and 5 mm. This attributes to the bactericidal property of silver nanoparticles in the composite membranes, where silver is a well known antibacterial material. It was found that, as the concentration of Al_2O_3 increases, the zone of inhibition decreases slightly, which is due to the decrease in exposure of silver nanoparticles present on the surface as Al_2O_3 is added to the membrane.

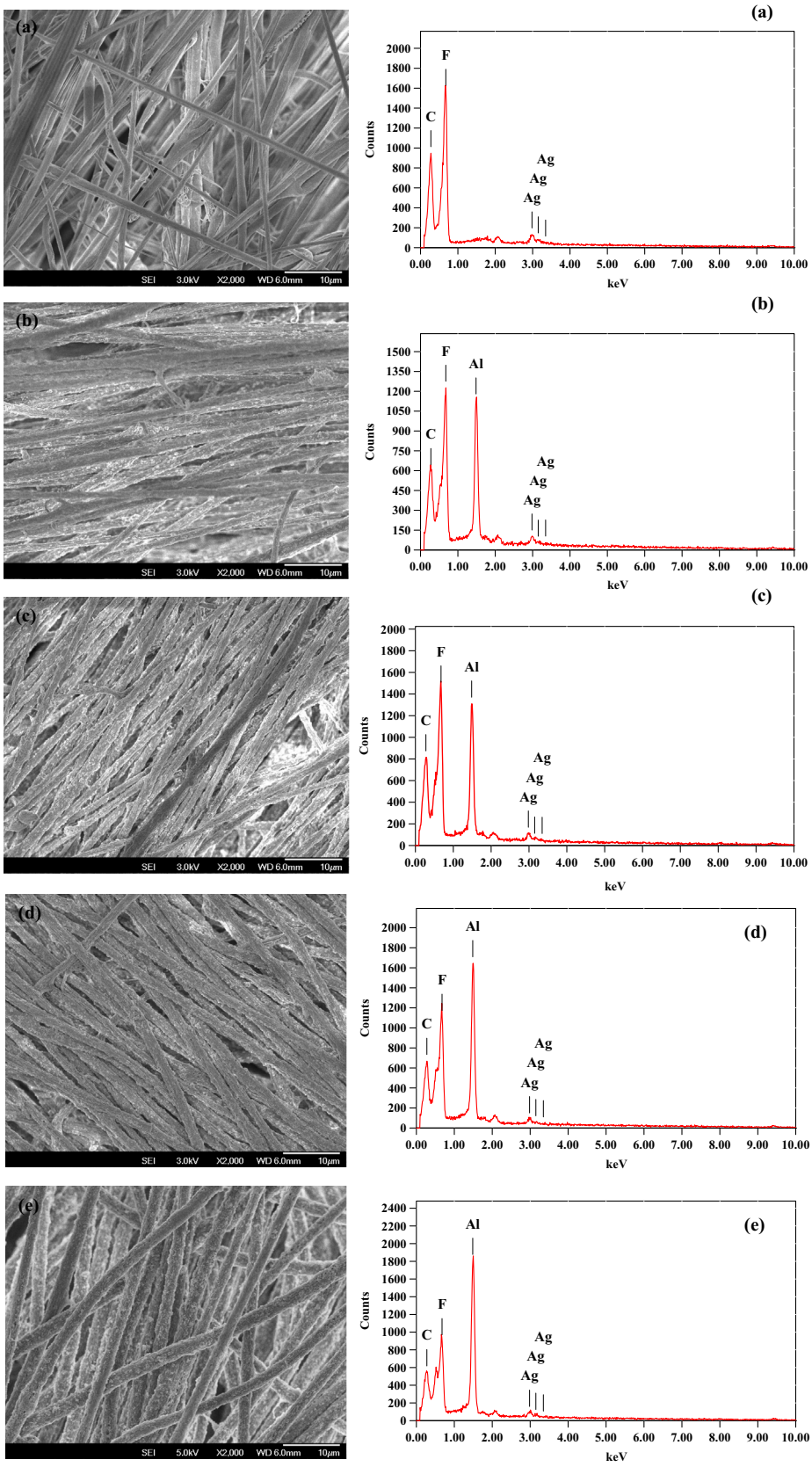

Fig. 2. FESEM (left) and EDS (right) images of electropsun PVDF–Ag–metal oxide membranes with (a) 0% Al_2O_3, (b) 2% Al_2O_3, (c) 4% Al_2O_3, (d) 6% Al_2O_3, (e) 8% Al_2O_3.

However, Al_2O_3 also has antibacterial property, but of less activity than the silver. It was also observed that the zone of inhibition hardly changed even if the samples were kept for about 1 week at room temperature, showing that the antibacterial property of the membrane is effective and durable. In contrast, the PDVF membrane exhibits no zone of inhibition under the same condi-

Table 1
Characterization of PVDF (control), PVDF–Ag–0% Al_2O_3 (M1), PVDF–Ag–2% Al_2O_3 (M2), PVDF–Ag–4% Al_2O_3 (M3), PVDF–Ag–6% Al_2O_3 (M4), PVDF–8% Al_2O_3 (M5) membranes.

Membrane samples	Average fiber diameter (μm)	Average thickness (μm)	Average pore size (μm)	Contact angle (°)	Filter resistance, R_f (Pa.s/m)
PVDF (control)	0.42 ± 0.12	50.4	0.56	139.4 ± 0.7	633.8 ± 17.61
M1	0.52 ± 0.13	51.4	0.48	137.4 ± 1.2	651.41 ± 35.21
M2	1.19 ± 0.97	52.1	0.33	136.9 ± 0.9	661.97 ± 52.82
M3	1.48 ± 0.13	56.2	0.34	137.5 ± 0.4	669.01 ± 17.61
M4	1.67 ± 0.64	60.1	0.33	138.0 ± 0.1	683.1 ± 35.21
M5	1.85 ± 0.19	62.9	0.36	137.0 ± 1.1	704.23 ± 52.82

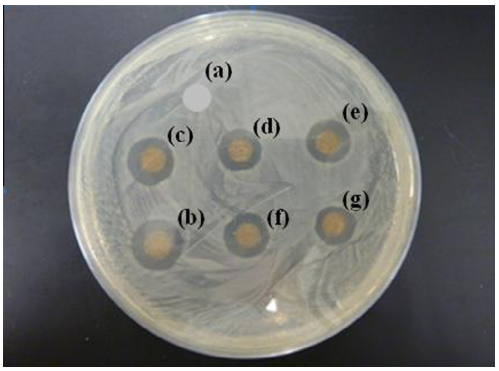

Fig. 3. Zone of Inhibition of (a) PVDF, (b) PVDF–Ag–0% Al_2O_3, (c) PVDF–Ag–2% Al_2O_3, (d) PVDF–Ag–4% Al_2O_3, (e) PVDF–Ag–6% Al_2O_3, (f) & (g) PVDF–Ag–8% Al_2O_3.

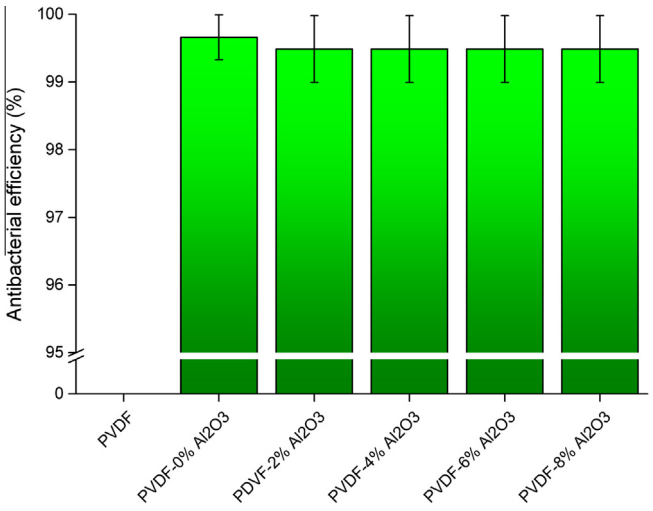

Fig. 4. Antibacterial efficiency percentage (%) of the nanofiber membranes.

tions and high bacterial growth near the sample was detected. These results indicated that the incorporation of Ag and Al_2O_3 nanoparticles have in turn incorporated the antibacterial property into the nanofiber composite membranes, to disinfect the biological pollutants in air.

3.2.2. Antibacterial efficiency test

In this test, the number of bacterial colonies (CFU) was counted after the incubation of the membranes in the bacterial solution. The counts were used to calculate the surviving number of bacteria. The degree of the antibacterial effect is the ratio of the reduction of bacterial colonies. This test was performed in triplicates and the antibacterial efficiency was found to be above 99% for all membrane samples except PDVF control which has no antibacterial activity as shown in Fig. 4. This proves that the composite nanofiber membranes are active against the *E. coli* bacteria. This is mainly because of the silver, which is well known for the antibacterial activity and so is used in several applications. The results clearly indicate that the silver and the metal oxide particles exhibit its own antibacterial activity. We also observe that the M1 membrane has an average antibacterial efficiency of 99.66%, which is more than the other membranes. This is attributed to the more number of silver nanoparticles on the surface of the membrane, while the other membranes take up space for the metal oxide on its surface. The zone of inhibition test result supports this as well. In this study, a homogenous solution containing silver and Al_2O_3 nanoparticles was used as the spinning solution. Besides being exposed on the

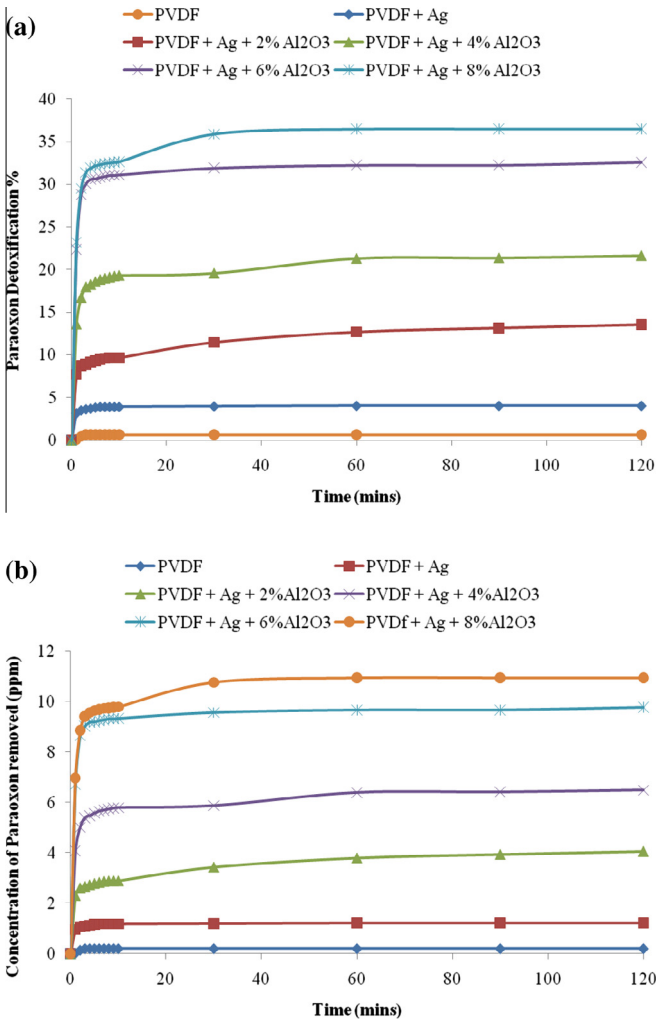

Fig. 5. Effect of membranes M1, M2, M3, M4, M5 and PVDF on (a) paraoxon detoxification percentage (b) concentration of paraoxon removed in ppm.

surface, silver particles are also embedded inside the nanofibers like the metal oxide nanoparticles that also have some antibacterial function. Some literature shows that the Ag^+ ions can be released from the inside of electrospun nanofibers [37,40,41]. Due to this, the nanoparticles present, the porous structure and high surface area of the nanofiber membranes is said to have an excellent antibacterial activity. The antibacterial activity of the membranes can also be increased or decreased by adjusting the composition of the silver and Al_2O_3 nanoparticles in the membrane. Thus, the prepared hybrid composite membranes with silver and Al_2O_3 nanoparticles incorporated, has a broad spectrum antimicrobial property that can kill biological pollutants in air.

3.3. Detoxification studies

The prepared hybrid hydrophobic composite membranes and the control were tested for the hydrolysis of nerve agent simulant namely paraoxon in heptane. The detoxification of the chemical pollutant Paraoxon occurs by hydrolysis into its simplest forms. Fig. 5(a) shows the trend of decrease in the concentration for paraoxon at 268 nm as the time increases from 0 to 120 min. The sample membranes and the control membrane were measured for the optical density using the UV spectrophotometer after stirring with paraoxon for the required time intervals. The measurements were then compared for the relative rate of hydrolysis of paraoxon. It was found that the membrane M5 reduces the paraoxon concentration relatively more than the other membranes. However from the figure, we can see that, as the concentration of Al_2O_3 increases, the decrease in paraoxon concentration increases constantly until 120 min. Fig. 5(b) shows the detoxification efficiency of the membranes along with the control sample. The detoxification efficiency was found to be increasing as the concentration of the Al_2O_3 increases. It was found that the efficiency increases to 36.47% for M5 membrane which is about 3.89% higher than M4, 14.85% higher than M3, 22.92% higher than M2, 32.41% higher than M1 and 35.81% higher than the PVDF control membrane. Thus the increased orders of the reactivity of the membranes are found to be PVDF < PVDF–Ag–0% Al_2O_3 < PVDF–Ag–2% Al_2O_3 < PVDF–Ag–4% Al_2O_3 < PVDF–Ag–6% Al_2O_3 < PVDF–Ag–8% Al_2O_3. This proves that the PVDF–Ag–8% Al_2O_3 membrane is highly active against the paraoxon showing about 36.47% detoxification. Further, increased rate of hydrolysis of paraoxon can be achieved by increasing the amount of membrane tested or increasing the initial metal oxide concentration in the electrospun membranes. Thus, the hybrid composite membranes containing Al_2O_3 can be used to detoxify the chemical pollutants present in the environment.

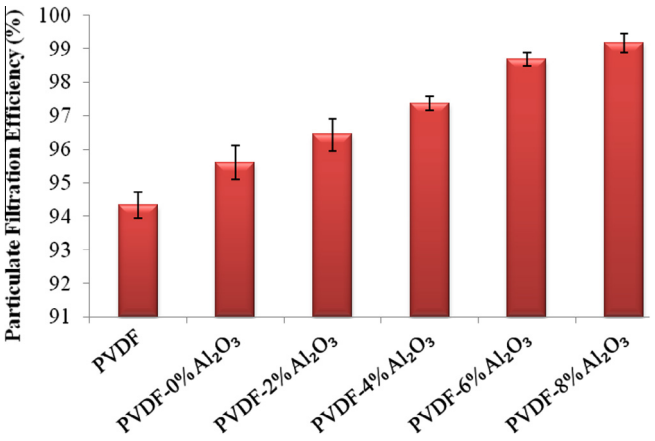

Fig. 6. Effect of membranes M1, M2, M3, M4, M5 and PVDF on particulate filtration efficiency in percentage.

3.4. Particulate filtration efficiency (PFE)

The aerosol testing equipment was used to find out the PFE of the membranes. Fig. 6 shows the experimental filtration efficiencies of the nascent and nanoparticle loaded membranes at a face velocity of 26.67 cm/s and a flow rate of 32 Lpm. The M5 membrane is found to be highly efficient in filtering 0.36 micron size particles and is 99.17% efficient, which is 0.49%, 1.81%, 2.74%, 3.57% and 4.84% higher than the M4, M3, M2, M1 and nascent PVDF membrane respectively. The aerosol test was conducted in trials and the average particle filtration efficiency was calculated. Thus, the increasing order of the PFE of the membranes are found to be PVDF < PVDF–Ag–0% Al_2O_3 < PVDF–Ag–2% Al_2O_3 < PVDF–Ag–4% Al_2O_3 < PVDF–Ag–6% Al_2O_3 < PVDF–Ag–8% Al_2O_3. This trend is due to the increase in the thickness of the membrane and the reduced pore size due to the addition of Al_2O_3 nanoparticles on to the membranes and hence the PFE increases with increasing concentration of Al_2O_3. This is evident from Table 1.

3.5. Filter resistance

The filter resistances (in Pa.s/m) of the developed composite membranes for an air flow velocity of 28.4 cm/s were given in Table 1. It was found that the filter/membrane resistance increased with increasing Al_2O_3 concentration. This due to the decreasing pore size and increasing thickness of the membrane, that provides higher retention of the particles and thus increasing the filter resistance. However, the production methods and the functional compounds for these membranes can be optimized to further reduce the filter resistance.

4. Conclusions

We have fabricated nanofibrous PVDF–metal oxide composite membranes for air filtration using silver and Al_2O_3 nanoparticles by electrospinning technique to evaluate the antimicrobial disinfection and the chemical detoxification functionalities respectively. The membrane structure, pore size, contact angle and resistance were shown to provide good air permeability and thus the membranes are suitable for air filtration applications. The antimicrobial and the detoxification efficiency of the membranes were also studied to show that the functionalized membrane can kill the pathogens and detoxify the chemical compounds that come into contact with them, which is an added functionality to the air filtration membranes. The detoxification and PFE efficiency of PVDF–Ag–8% Al_2O_3 membrane is the highest when compared to the other hybrid composite membranes. The increase in removal efficiency by the best performing filter was compensated by an increase in filter resistance of approximately 10% over the unmodified filters. The filter resistance can be further reduced by adjusting the structure of the membrane and optimizing the attachment of the nanoparticles on the filter fibers.

Acknowledgement

The authors would like to acknowledge the National Research Foundation (NRF), Singapore for funding of this work with Grant No. NRFTRD1S0017.

References

[1] Q. Xavier, A. Andres, R. Sergio, P. Felicia, M. Enrique, R.R. Carmen, Monitoring of PM10 and PM2.5 around primary particulate anthropogenic emission sources, Atmos. Environ. 35 (2001) 845–858.

[2] R. Sergio, Q. Xavier, A. Andres, M.V. Maria, A. Marta, M. Enrique, C.R. Ruiz, Comparative PM10–PM2.5 source contribution study at rural, urban and industrial sites during PM episodes in Eastern Spain, Sci. Total Environ. 328 (2004) 95–113.

[3] Y. Li, K. Xiao, J. Luo, J. Lee, S. Pan, K.S. Lam, A novel size-tunable nanocarrier system for targeted anticancer drug delivery, J. Control. Release 144 (2010) 314.

[4] P. Claus, H. Hofmeister, Electron microscopy and catalytic study of silver catalysts: structure sensitivity of the hydrogenation of crotonaldehyde, J. Phys. Chem. B 103 (1999) 2766–2775.

[5] Z.J. Jiang, C.Y. Liu, L.W. Sun, Catalytic properties of silver nanoparticles supported on silica spheres, J. Phys. Chem. B 109 (2005) 1730–1735.

[6] P. Mulvaney, Surface plasmon spectroscopy of nanosized metal particles, Langmuir 12 (1996) 788–800.

[7] R.C. Jin, Y.W. Cao, C.A. Mirkin, K.L. Kelly, G.C. Schatz, J.G. Zheng, Photoinduced conversion of silver nanospheres to nanoprisms, Science 294 (2001) 1901–1903.

[8] A. Callegari, D. Tonti, M. Chergui, Photochemically grown silver nanoparticles with wavelength-controlled size and shape, Nano Lett. 3 (2003) 1565–1568.

[9] S. Pal, Y.K. Tak, J.M. Song, Does the antibacterial activity of silver nanoparticles depend on the shape of the nanoparticle? A study of the gram-negative bacterium *Escherichia col*, Appl. Environ. Microbiol. 73 (2007) 1712–1720.

[10] L. Zhang, J.C. Yu, H.Y. Yip, Q. Li, K.W. Kwong, A. Xu, P.K. Wong, Ambient light reduction strategy to synthesize silver nanoparticles and silver-coated TiO_2 with enhanced photocatalytic and bacterial activities, Langmuir 19 (2003) 10372–10380.

[11] J.R. Morones, J.L. Elechiguerra, A. Camacho, K. Holt, J.B. Kouri, J.T. Ramirez, M.J. Yacaman, The bacterial effect of silver nanoparticles, Nanotechnology 16 (2005) 2346–2353.

[12] A. Panacek, L. Kvitek, R. Prucek, M. Kolar, R. Vecerova, N. Pizurova, V.K. Sharma, N. Tat'jana, Z. Zboril, Silver colloid nanoparticles: synthesis, characterization, and their antibacterial activity, J. Phys. Chem. B 110 (2006) 1624–16248.

[13] C. Hu, Y.Q. Lan, J.H. Qu, X.X. Hu, A.M. Wang, Ag/AgBr/TiO_2 visible light photocatalyst for destruction of azodyes and bacteria, J. Phys. Chem. B 110 (2006) 4066–4072.

[14] M. Jin, X.T. Zhang, S. Nishimoto, Z.Y. Liu, D.A. Tryk, A.V. Emeline, T. Murakami, A. Fujishima, Light-stimulated composition conversion in TiO_2-based nanofibers, J. Phys. Chem. C 111 (2007) 658–665.

[15] G. Rena, D. Hu, E.W.C. Cheng, M.A. Vargas-Reus, P. Reip, R.P. Allaker, Characterization of copper oxide nanoparticles for antimicrobial applications, Int. J. Antimicrob. Agents 33 (2009) 587–590.

[16] N. Jones, B. Ray, K.T. Ranjit, A.C. Manna, Antibacterial activity of ZnO particle suspensions on a broad spectrum of microorganisms, FEMS Microbiol. Lett. 279 (2008) 71–76.

[17] R. Ramakrishna, S. Sundarrajan, Y. Liu, R.S. Barhate, N.L. Lala, S. Ramakrishna, Functionalized polymer nanofiber membranes for protection from chemical warfare stimulants, Nanotechnology 17 (2006) 2947–2953.

[18] G.W. Wagner, Y.C. Yang, Rapid nucleophilic oxidative decontamination of chemical warfare agent, Ind. Eng. Chem. 41 (2002) 1925–1928.

[19] G. Amitai, R. Adani, M. Hershkovitz, P. Bel, I. Rabinovitz, H. Meshulam, Degradation of VX and sulfur mustard by enzymatic haloperoxidation, J. Appl. Toxicol. 23 (2003) 225–233.

[20] C.R. Reigenbach, S.R. Livingston, D. Kumar, C.C. Landry, V-doped APMS: synthesis, characterization, and catalytic studies on oxidation of 2-chloroethyl ethylsulfide, Chem. Mater. 17 (2005) 5580–5586.

[21] T. Cassagne, Comparative evaluation of oxidizing and nucleophilic properties of some α-nucleophiles, J. Chem. Res. 7 (2002) 336–338.

[22] K. Kuca, J. Kassa, A comparison of the ability of a new bispyridinium oxime-1-(4-hydroxyiminomethylpyridinium)-4-(4-carbamoylpyridinium) butane dibromide and currently used oximes to reactivate nerve agent-inhibited rat brain acetylcholinesterase by in vitro methods, J. Enzyme Inhib. Med. Chem. 18 (2003) 6.

[23] (a) K.K. Klabunde, J. Stark, O. Koper, C. Mohs, D.G. Park, S. Decker, Y. Jiang, I. Lagadic, D. Zhang, Nanocrystals as stoichiometric reagents with unique surface chemistry, J. Phys. Chem. 100 (1996) 12142–12153;
(b) J.V. Stark, D.G. Park, I. Lagadic, K.J. Klabunde, Nanoscale metal oxide particles/clusters as chemical reagents. Unique surface chemistry on magnesium oxide as shown by enhanced adsorption of acid gases (sulfur dioxide and carbon dioxide) and pressure dependence, J. Mater. Chem. 8 (1996) 1904–1912.

[24] S. Sundarrajan, S. Ramakrishna, Fabrication of nanocomposite membranes from nanofibers and nanoparticles for protection against chemical warfare stimulants, J. Mater. Sci. 42 (2006) 8400–8407.

[25] http://www.deconsolutions.com/pdf_Files/TECHNICAL%20REPORT%20MOD2003-1012 G.pdf.

[26] Q.L. Li, S. Mahendra, D.Y. Lyon, L. Brunet, M.V. Liga, D. Li, P.J.J. Alvarez, Antimicrobial nanomaterials for water disinfection and microbial control: potential applications and implications, Water Res. 42 (2008) 4591–4602.

[27] N. Ichinose, Superfine Particle Technology, Springer, Berlin, 1992.

[28] D.M. Cox, R.O. Brickman, K. Creegan, A. Kaldor, Clusters and Cluster-Assembled Materials, in: R.S. Nelson (Ed.), Materials Research Society, 1991, p. 43.

[29] O. Koper, E. Lucas, K.J. Klabunde, Development of reactive topical skin protectants against sulfur mustard and nerve agents, J. Appl. Toxicol. 19 (1999) 59–70.

[30] K.J. Klabunde, Nanoscale Materials in Chemistry, Wiley Interscience, New York, 2001.

[31] W.W. George, W.B. Philip, K. Olga, J.K. Kenneth, Reactions of VX, GD, HD with nanosize MgO, J. Phys. Chem. B 103 (1999) 3225–3228.

[32] R. Balamurugan, S. Sundarrajan, S. Ramakrishna, Recent trends in nanofibrous membranes and their suitability for air and water filtrations, Membranes 1 (2011) 232–248.

[33] W.K. Son, J.H. Youk, W.H. Park, Antimicrobial cellulose acetate nanofibers containing silver nanoparticles, Carbohydr. Polym. 65 (2006) 430–434.

[34] N.L. Lala, R. Ramaseshan, L. Bojun, S. Sundarrajan, R.S. Barhate, L. Ying-Jun, S. Ramakrishna, Fabrication of nanofibers with antimicrobial functionality used as filters: protection against bacterial contaminants, Biotechnol. Bioeng. 97 (2007) 1357–1365.

[35] Q.B. Yang, D.M. Li, Y.L. Hong, Z.Y. Li, C. Wang, S.L. Qui, Y. Wei, Preparation and characterization of a PAN nanofiber containing Ag nanoparticles via electrospining, Synth. Met. 137 (2003) 973–974.

[36] Z. Li, H. Huang, T. Shang, F. Yang, W. Zheng, C. Wang, S.K. Manohar, Facile synthesis of single-crystal and controllable sized silver nanoparticles on the surfaces of polyacrylonitrile nanofibers, Nanotechnology 17 (2006) 917–920.

[37] Y. Wu, W. Jia, Q. An, Y. Liu, J. Chen, G. Li, Multiaction antibacterial nanofibrous membranes fabricated by electrospinning: an excellent system for antibacterial applications, Nanotechnology 20 (2009) 245101.

[38] S. Kaur, Z. Ma, R. Gopal, G. Singh, S. Ramakrishna, T. Matsuura, Plasma-induced graft copolymerization of poly(methacrylic acid) on electrospun poly(vinylidene fluoride) nanofiber membrane, Langmuir 23 (2007) 13085–13092.

[39] M. Suzuki, A. Kishida, H. Iwata, Y. Ikada, Graft copolymerization of acrylamide onto a polyethylene surface pretreated with glow discharge, Macromolecules 19 (1986) 1804–1808.

[40] M. Abdulkareem, Z.H. Sun, H. Khadijah, M. Amy, E. Daniel, H.R. Darrell, A.T. Claire, J.Y. Wiley, Silver(I)-imidazole cyclophane gem-diol complexes encapsulated by electrospun tecophilic nanofibers: formation of nanosilver particles and antimicrobial activity, J. Am. Chem. Soc. 127 (2005) 2285–2291.

[41] W.P. Huang, Y.Q. Tang, Y. Koltypin, A. Gedanken, Selective synthesis of anatase and rutile via ultrasound irradiation, Chem. Commun. 15 (2000) 1415–1416.